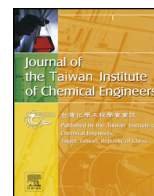




Contents lists available at [SciVerse ScienceDirect](http://www.sciencedirect.com)

Journal of the Taiwan Institute of Chemical Engineers

journal homepage: [www.elsevier.com/locate/jtice](http://www.elsevier.com/locate/jtice)



# Optimizing decolorization of Methylene Blue and Methyl Orange dye by pulsed discharged plasma in water using response surface methodology

Yanping Jin<sup>a</sup>, Yunhai Wu<sup>a</sup>, Julin Cao<sup>b</sup>, Yuning Wu<sup>c,\*</sup>

<sup>a</sup>Key Laboratory of Integrated Regulation and Resources Development of Shallow Lakes, Ministry of Education, Hohai University, Nanjing 210098, China

<sup>b</sup>College of Environment, Hohai University, Nanjing 210098, China

<sup>c</sup>Department of Chemistry, Hanshan Normal University, Chaozhou, China

## ARTICLE INFO

### Article history:

Received 10 April 2013

Received in revised form 4 June 2013

Accepted 5 June 2013

Available online xxx

### Keywords:

Methyl Orange

Methylene Blue

Optimization

Pulsed discharged plasma

Response surface methodology

## ABSTRACT

Dye removal using pulsed discharged plasma in water requires a proper process parametric study to determine its optimal performance characteristics. Response surface methodology was used to find out the major factors influencing Methylene Blue (MB) and Methyl Orange (MO) removal efficiency and the interactions between these factors (ultrasonic power, gas flow rate, and electrode spacing), and optimized the operating variables as well. Regression analysis showed good fit of the experimental data to the second-order polynomial model with coefficient of determination value of 0.9960 and 0.9861 for MB and MO, respectively. Under the experimental conditions: gas flow rate 0.1 m<sup>3</sup>/h, electrode spacing 10 mm for all the dyes, and ultrasonic power 80 and 90 W for MB and MO, the highest dye removal efficiency were achieved 94.5% and 80.2% for MB and MO. The optimal results suggested that pulsed discharged plasma oxidation process was a rapid, efficient, and low energy consumption technique to remove the dyes wastewater.

© 2013 Taiwan Institute of Chemical Engineers. Published by Elsevier B.V. All rights reserved.

## 1. Introduction

The increasing use of dyes in various industrial applications has resulted in the discharge of toxic dye effluents into the water streams causing serious environmental pollution [1]. Moreover, many dyes are difficult to degrade, as they are generally stable to light, oxidizing agent and are resistant to aerobic digestion [2]. Hence, the removal of dyes from process or waste effluents becomes environmentally important.

The conventional methods, such as biological oxidation, chemical coagulation and adsorption have been applied for dye removal from water and wastewaters [3,4]. Biological methods are generally cheap and simple to apply and are currently used to remove organics and color from dyeing and textile wastewater. However, this dyeing wastewater cannot be readily degraded by the conventional biological processes, e.g., activated sludge process, because the structures of most commercial dye compounds are generally very complex and many dyes are non-biodegradable due to their chemical nature, molecular size and result in sludge bulking [5]. Although dyestuffs and color materials

in wastewater can be effectively destroyed by wet oxidation [6], adsorption using activated carbon [7,8], and electrocoagulation using Al or Fe soluble electrodes [9], the costs of these methods are relatively high.

Therefore, novel methods, especially advanced oxidation processes (AOPs), have been applied for treating dye wastewaters that are non-biodegradable and toxic to microorganisms [10]. Researchers have tested various processes, such as photo oxidative process, electrochemical process, H<sub>2</sub>O<sub>2</sub> oxidation, ultrasonic process, Fenton and Fenton-like [11–14], ozone oxidation [15–17], and plasma process. More recently, among the AOPs, the pulsed discharged plasma in water has been considered to be an applicable method for the removal of organic pollutants from wastewater [18–20]. Pulsed discharged plasma in water is efficient in the formation of chemically active species such as OH, H, O, O<sub>3</sub>, and H<sub>2</sub>O<sub>2</sub>. Most of these species are among the strongest oxidizing agents. The effect plays an important role in destroying harmful organic pollutants in wastewater [21]. However, in the plasma process, many factors such as pH, ultrasonic power, the electrolyte concentration, gas flow rate, electrode spacing, and the application time influence the process efficiency. The process efficiency may be increased by the optimization of these factors. In conventional multifactor experiments, optimization is usually carried out by varying a single factor while keeping all the other factors fixed at a

\* Corresponding author. Tel.: +86 7682318681; fax: +86 7682318681.

E-mail address: [jinyanping0408@yahoo.cn](mailto:jinyanping0408@yahoo.cn) (Y. Wu).

specific set of condition. This method is time-consuming and incapable of effective optimization. Recently, response surface methodology (RSM) has been employed to optimize and understand the performance of complex systems [22]. By application of RSM, it is possible to evaluate the interactions of possible influencing factors on treatment efficiency with a limited of planned experiments [23–25].

In the present study, RSM with Box–Behnken design (BBD), Design Expert Version 8.0.6 program (Stat-Ease Inc., Minneapolis, USA), was employed for the optimization of Methylene Blue (MB) and Methyl Orange (MO) by pulsed discharged plasma. The main objectives were to optimize the process and investigate the factors that influence the removal efficiency. Dye removal efficiency was chosen as the dependent factor (response) and the ultrasonic power, gas flow rate, and electrode spacing were selected as process variables. The optimal conditions for dyes removal were also determined from the model obtained via experimental data.

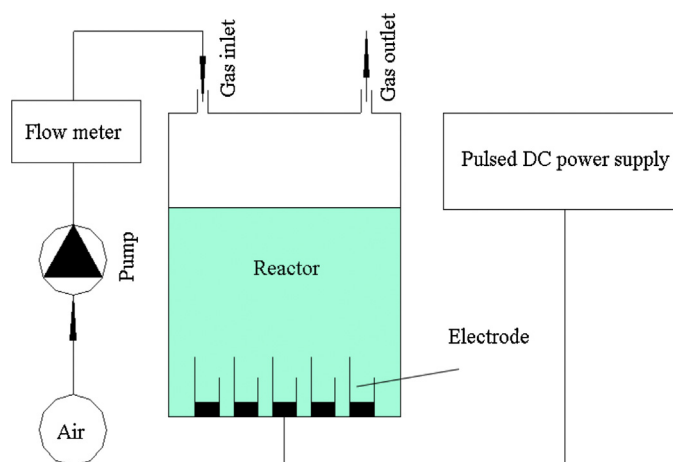


Fig. 2. Schematic diagram of the experimental apparatus.

## 2. Materials and methods

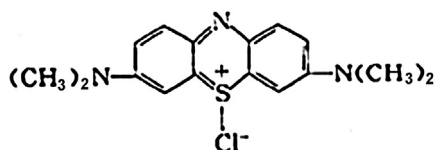
### 2.1. Materials

All dyes used in this study were purchased from Nanjing RuiTai Chemical Reagents, Ltd. The structures of dyes MB and MO were shown in Fig. 1. Double distilled water was used in all the experiments, to prepare the stock solution of MB and MO. Working solutions ( $1.40 \times 10^{-6}$  M) were prepared by suitable dilution of the stock solutions. The initial solution pH was adjusted by added a little amount of 0.1 M NaOH or 0.1 M HCl into the solution until the conductivity becomes  $400 \pm 50 \mu\text{s/cm}$ . Since the conductivity greatly affect the formation of plasma discharged in water, the initial conductivity should be kept constant in all experiment [21].

### 2.2. Experimental procedure

The schematic diagram of experimental apparatus is shown in Fig. 2. Plasma was generated from Plasma Power and pulse modulator (EcoTopia Science Institute, Nagoya University, Japan). Operation conditions: pulse repetition frequency and pulse width were set at 0.1–30 kHz and 0–2  $\mu\text{s}$ , respectively. And discharge state was controlled by the value of output voltage in 80–100 V. The processing reactor, made of stainless steel, had a diameter of 480 mm and a height of 600 mm. Air was often used as bubbling gas with the purpose of improving the liquid discharge performance in some pulsed high-voltage discharge system [26]. The process gas (air) was introduced into the active volume of the plasma via a gas flow control system. The pulsed discharge reactor used in this work was done with bipolar pulse DC power supply.

### Methylene Blue



### Methyl Orange

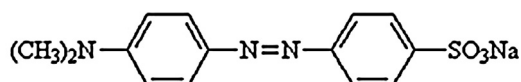


Fig. 1. Chemical structures of the two utilized dyes.

When the plasma source was on, the press was measured by a capacitive vacuum gauge. Samples were introduced by a load lock system and placed on a grounded aluminum holder near the center of the processing reactor. The electrodes used in experiments were made of stainless (1.5 mm). The ultrasonic power was estimated by measuring the applied voltages, discharge current and the pulse repetition rate. The values of pulsed output voltage and current were measured using a digital oscilloscope (Lecroy LT264) with a high voltage probe (INC P150-GL/5 k) and a current transducer (Pearson Electronic M411). The discharge power *i.e.*  $V \times I$  could be calculated from the product of the measured pulse voltage ( $V$ ) and the discharge current ( $I$ ).

Samples were taken periodically from the reactor and then analyzed immediately with UV-vis spectrophotometer (Shimadzu, Japan) with wavelength of 660 nm and 440 nm for MB and MO solution, respectively. The flow rate of the dye solution was 100 mL/min. Samples were taken from the reactor from the sampling traps to determine absorbance prior to the reaction. At predetermined time of 30 min, 10 mL samples were withdrawn from the reactor and analyzed to determine absorbance. The dye removal efficiency can be calculated based on the following equation:

$$\eta = \frac{\alpha_0 - \alpha_t}{\alpha_0} \times 100\% \quad (1)$$

where  $\alpha_0$  (mg/L) was the initial concentration and  $\alpha_t$  (mg/L) was the concentration at discharge time  $t$  (min).

### 2.3. Response surface methodology

RSM is a collection of statistical and mathematical techniques useful for developing, improving, and optimizing process. The main objective of RSM is to determine the optimum operational conditions for the systems or to determine a region that satisfies the operating specifications [27]. The main advantage of RSM is the reduced number of experimental trials needed to evaluate multiple parameters and their interactions. Its great applications particularly have been in situations where a large number of variables influencing the system feature. This feature termed as the response and normally measured on a continuous scale, which represents the most important function of the systems [28].

### 2.4. Experimental design

A 3-factor, 3-level factorial Box–Behnken design (BBD) was employed to investigate the effects of selected variables. BBD,

**Table 1**

The experimental domain factor and level for the Box–Behnken design.

Factors		Range and levels (coded)		
		−1	0	+1
Ultrasonic power (W)	A	60	80	100
Gas flow rate (m <sup>3</sup> /h)	B	0.04	0.07	0.10
Electrode spacing (mm)	C	10	20	30

which is a widely used form of RSM, specially made to require only 3 levels, coded as −1, 0, and +1. BBD is an independent, rotatable or nearly rotatable quadratic design (contains no embedded factorial or fractional factorial design) in which the treatment combinations are at the midpoints of the edges of the process space and at the center [29]. For statistical calculations, the variable  $X_i$  was coded as  $Z_i$  according to the following equation [30,31]:

$$Z_i = \frac{X_i - X_0}{\Delta X_i} \quad (2)$$

where  $X_i$  is the real value of the  $i$ th independent variable,  $X_0$  is the real value of an independent variable at the center point, and  $\Delta X_i$  is the step change.

The variables (independent factors) used in this study were: ultrasonic power, gas flow rate, and electrode spacing. MB and MO removal efficiency ( $Y(\%)$ ) was considered as the dependent factor (response). The actual values of process variables and their variation limits were selected based on the values obtained in preliminary experiments and coded as shown in Table 1. The observations were fitted to a second-order polynomial model as given below [32,33]:

$$Y(\%) = \beta_0 + \sum_{i=1}^n \beta_i X_i + \sum_{i=1}^n \beta_{ii} X_i^2 + \sum_{i=1}^{n-1} \sum_{j=2}^n \beta_{ij} X_i X_j + \varepsilon \quad (3)$$

where  $\beta_0$  is the intercept term,  $\beta_i$ ,  $\beta_{ii}$ , and  $\beta_{ij}$  are the regression coefficients and  $X_i$ ,  $X_j$  represent the coded values of independent variables, and  $\varepsilon$  is the random error [34]. The optimum values of the selected variables were obtained by solving the regression equation at desired values of the process responses as the optimization criteria. The data were subjected to analysis of variance and the coefficient of regression ( $R^2$ ) was calculated to find out the goodness of fit of the model [24].

**Table 2**

The Box–Behnken design matrix for experimental design, observed and predicted response for removal of MB and MO.

Run order	Real (coded) values			Response ( $Y(\%)$ )			
	A	B	C	MB		MO	
				Observed value	Predicted value	Observed value	Predicted value
1	60(−1)	0.04(−1)	20(0)	43.3	45.6	24.0	25.0
2	100(1)	0.04(−1)	20(0)	54.0	53.6	38.5	35.5
3	60(−1)	0.1(1)	20(0)	62.0	62.4	40.5	43.5
4	100(1)	0.1(1)	20(0)	86.2	84.0	63.7	62.7
5	60(−1)	0.07(0)	10(−1)	78.3	77.1	58.4	55.1
6	100(1)	0.07(0)	10(−1)	93.7	95.1	72.0	72.7
7	60(−1)	0.07(0)	30(1)	43.1	41.7	25.0	24.3
8	100(1)	0.07(0)	30(1)	52	53.2	33.1	36.4
9	80(0)	0.04(−1)	10(−1)	73.5	72.5	49.2	51.5
10	80(0)	0.1(1)	10(−1)	96.8	94.5	76.7	77.0
11	80(0)	0.04(−1)	30(1)	36.2	35.4	21.0	20.7
12	80(0)	0.1(1)	30(1)	56.4	57.4	43.2	40.9
13	80(0)	0.07(0)	20(0)	80.7	80.7	52.2	51.4
14	80(0)	0.07(0)	20(0)	81	80.7	51.9	51.4
15	80(0)	0.07(0)	20(0)	81.4	80.7	50.8	51.4
16	80(0)	0.07(0)	20(0)	80.7	80.7	50.5	51.4
17	80(0)	0.07(0)	20(0)	79.7	80.7	51.6	51.4

### 3. Results and discussion

#### 3.1. Fitting of process models and statistical analysis

The experimental results were evaluated by the dependent variables of dye removal efficiency ( $Y(\%)$ ), using Design Expert software approximating functions. The results are obtained with the experimental design that was aimed at identifying the best levels of the selected variables, *i.e.* ultrasonic power (60–100 W), gas flow rate (0.04–0.10 m<sup>3</sup>/h), and electrode spacing (10–30 mm) (Table 2). Polynomial regression modeling was performed between the response variable and the corresponding coded values (A, B, C) of the three different process variables, and finally, the best fitted model equations were obtained in Eqs. (4) and (5):

$$\text{MB } Y(\%) = 80.70 + 7.40A + 11.80B - 19.33C + 3.37AB - 9.14A^2 - 10.19B^2 - 4.79C^2 \quad (4)$$

$$\text{MO } Y(\%) = 51.40 + 7.43A + 11.43B - 16.75C - 5.06A^2 - 4.66B^2 \quad (5)$$

In Eqs. (4) and (5), A, B, and C are corresponding to independent variables of ultrasonic power, gas flow rate, and electrode spacing, respectively. Positive values in both equations indicate that these terms increase the response, and the negative values decrease the response [35].

The analysis of variance (ANOVA) is a statistical technique that subdivides the total variation in a set of data into component parts associated with specific sources of variation for the purpose of testing hypotheses on the parameters of the model [36]. ANOVA results of these quadratic models presented in Table 3 indicated that these quadratic models can be used to navigate the design space. According to ANOVA, the Fisher  $F$  values for all regressions were higher. The large value of  $F$  indicates that most of the variation in the response can be explained by the regression equation. The associated  $p$  value is used to estimate whether  $F$  is large enough to indicate statistical significance. The Prob  $> F$  value ( $<0.0001$ ) of the model are lower than 0.05 (*i.e.*  $\alpha = 0.05$ ) indicating that the quadratic model was statistically significant [13], whereas values greater than 0.1000 indicate the model terms are not significant. The model  $F$ -values of 192.32 and 55.05 for MB and MO imply that the terms in the model have a significant effect on the response (Table 3). Adequate precision measures the signal to noise ratio and a ratio greater than 4 is desirable. In the present

**Table 3**  
Analysis of variance (ANOVA) variables fitted to quadratic polynomial models.

Source	Sum of squares		df	Mean square		F-value		Prob > F	
	MB	MO		MB	MO	MB	MO	MB	MO
Model	5575.77	3974.04	9	619.53	441.56	192.32	55.05	<0.0001	<0.0001
A	438.08	441.05	1	438.08	441.05	135.99	54.99	<0.0001	0.0001
B	1113.92	1044.25	1	1113.92	1044.25	345.78	130.19	<0.0001	<0.0001
C	2987.64	2244.50	1	2987.64	2244.50	927.43	279.84	<0.0001	<0.0001
AB	45.56	18.92	1	45.56	18.92	14.14	2.36	0.0071	0.1684
AC	10.56	7.56	1	10.56	7.56	3.28	0.94	0.1131	0.3639
BC	2.40	7.02	1	2.40	7.02	0.75	0.88	0.4164	0.3806
A <sup>2</sup>	351.55	107.91	1	351.55	107.91	109.13	13.45	<0.0001	0.0080
B <sup>2</sup>	436.99	91.53	1	436.99	91.53	135.65	11.41	<0.0001	0.0118
C <sup>2</sup>	96.51	2.61	1	96.51	2.61	29.96	0.33	0.0009	0.5861
Residual	22.55	56.15	7	3.22	8.02				
Lack of fit	20.97	54.05	3	6.99	18.02	17.70	34.31	0.0009	0.0026
Pure error	1.58	2.10	4	0.4	0.53				
Cor total	5598.32	4030.19	16						

$R^2_{MB} = 0.9960$ , (Adeq precision)<sub>MB</sub> = 45.221,  $R^2_{MO} = 0.9861$ , (Adeq precision)<sub>MO</sub> = 25.943.

situation a ratio of 45.221 for MB and 25.943 for MO obtained indicated adequate signals for the model to be used to navigate the design space. The fit of models are also evaluated by determination of coefficients ( $R^2$ ) and adjusted  $R^2$  ( $R^2_{adj}$ ). Actual responses are obtained by performing the experiments whereas predicted

responses are estimated from the model as proposed by the software [37]. The  $R^2$  is calculated by the ratio between the variation explained by the model and the total variation of the experimental data. Higher value of  $R^2$  is desirable as it is interpreted as the percentage of variability in the response explained by statistical model [38]. The values of  $R^2$  ( $R^2_{MB} = 0.9960$ ,  $R^2_{MO} = 0.9861$ ) and adjusted  $R^2$  ( $R^2_{adj,MB} = 0.9908$ ,  $R^2_{adj,MO} = 0.9682$ ) are close to 1, which are very high and indicate a high correlation between the observed and the predicted values. Therefore, the response surface model established in this study for predicting dyes removal using plasma was considered reasonable.

By applying the diagnostic plots provided by RSM (such as the predicted versus actual value plots), the adequacy of the modeled approximation can be estimated [39,40]. The predicted values of MB and MO removal efficiency obtained from the model were in good agreement with the obtained experimental data (Fig. 3).

### 3.2. Interactive effects of two variables

The sensitivity of the response to the two interacting variables can be included by the three-dimensional graphs by holding the other variable at the central values [41]. Variables giving quadratic and interaction terms with the largest absolute coefficients in the fitted models were chosen for the axes of the response surface plots to account for curvature of the surfaces. This was useful to visualize the relationship between the response and the level of each factor [42]. The influence of the three different process variables on the response factor are shown in the 3D response surface plots (Figs. 4 and 5a–c).

#### 3.2.1. Effects of ultrasonic power and gas flow rate

Figs. 4a,b and 5a,b show the combined effects of ultrasonic power and gas flow rate on dye removal at constant electrode spacing ( $C = 20$  mm) based on the fitted second-order polynomial equation. The both dye removal efficiency increased with increase of ultrasonic power ranging from 60 to 100 W as well as with gas flow rate ranging from 0.04 to 0.10 m<sup>3</sup>/h. A similar trend was observed by Lei *et al.* [43] in the study of the removal efficiency of 4-CP increased from 6.4% to 91.1% with the gas flow rate increasing from 0.2 to 0.5 m<sup>3</sup>/h using a novel pulsed high-voltage gas–liquid hybrid discharge continuous reactor. The reason was discharge intensity increased with the increase of ultrasonic power injected into reactor could increase the amount of active species (OH, O<sub>3</sub>, and H<sub>2</sub>O<sub>2</sub>) [44]. This led to the increase of oxidation amount of organic functional groups. In addition, discharge was firstly produced in gas phase; hence active species was engendered in

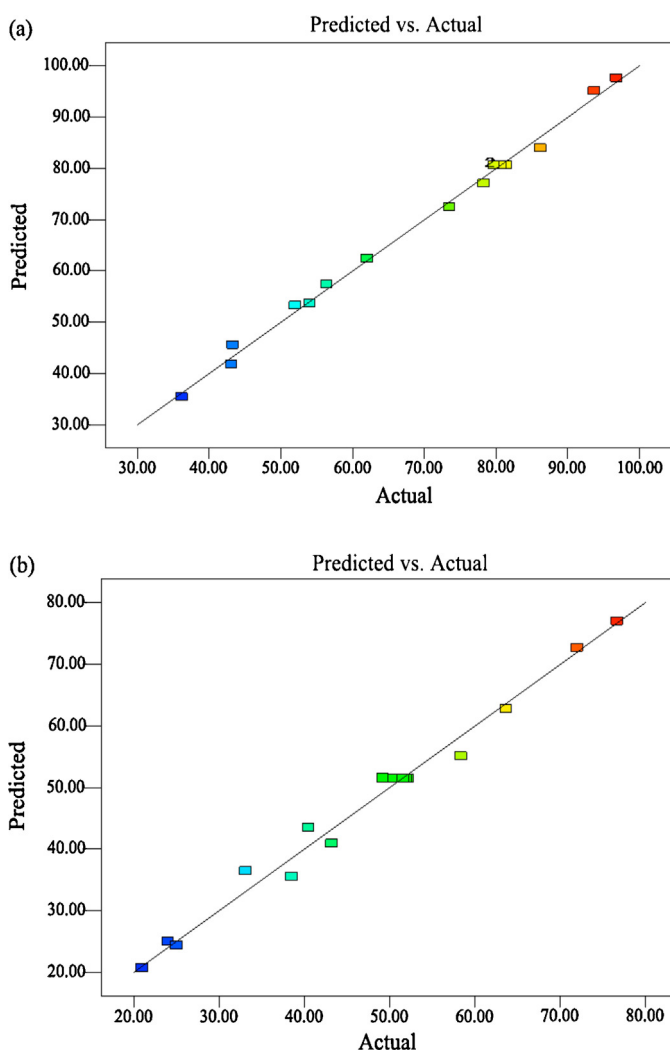
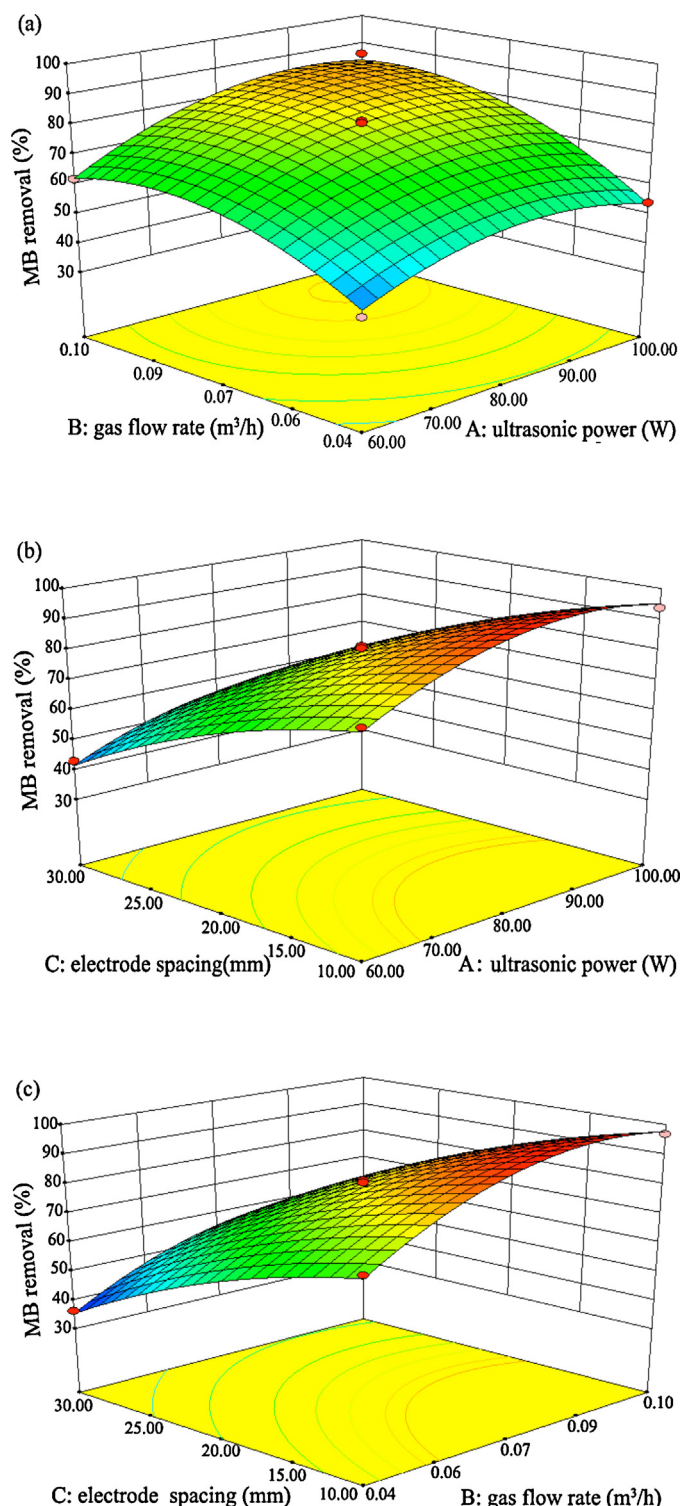


Fig. 3. Correlation of actual and predicted removal efficiency for (a) MB and (b) MO.



**Fig. 4.** Response surface plots for combined effect of (a) ultrasonic power and gas flow rate at constant electrode spacing of 20 mm, (b) ultrasonic power and electrode spacing at constant gas flow rate of 0.07 m<sup>3</sup>/h, and (c) gas flow rate and electrode spacing at constant ultrasonic power of 80 W on removal efficiency of MB.

gas phase. With the same discharge energy, the amount of the generated active species was also the same per unit electric energy.

According to the bubble theory of liquid breakdown, when gas was bubbled, there were more initial bubbles in water near the sharp point, and it was possible to accelerate electrons in the bubbles directly, leading to an increase in the mean-free-path length of the electrons [43]. Therefore more energetic electrons

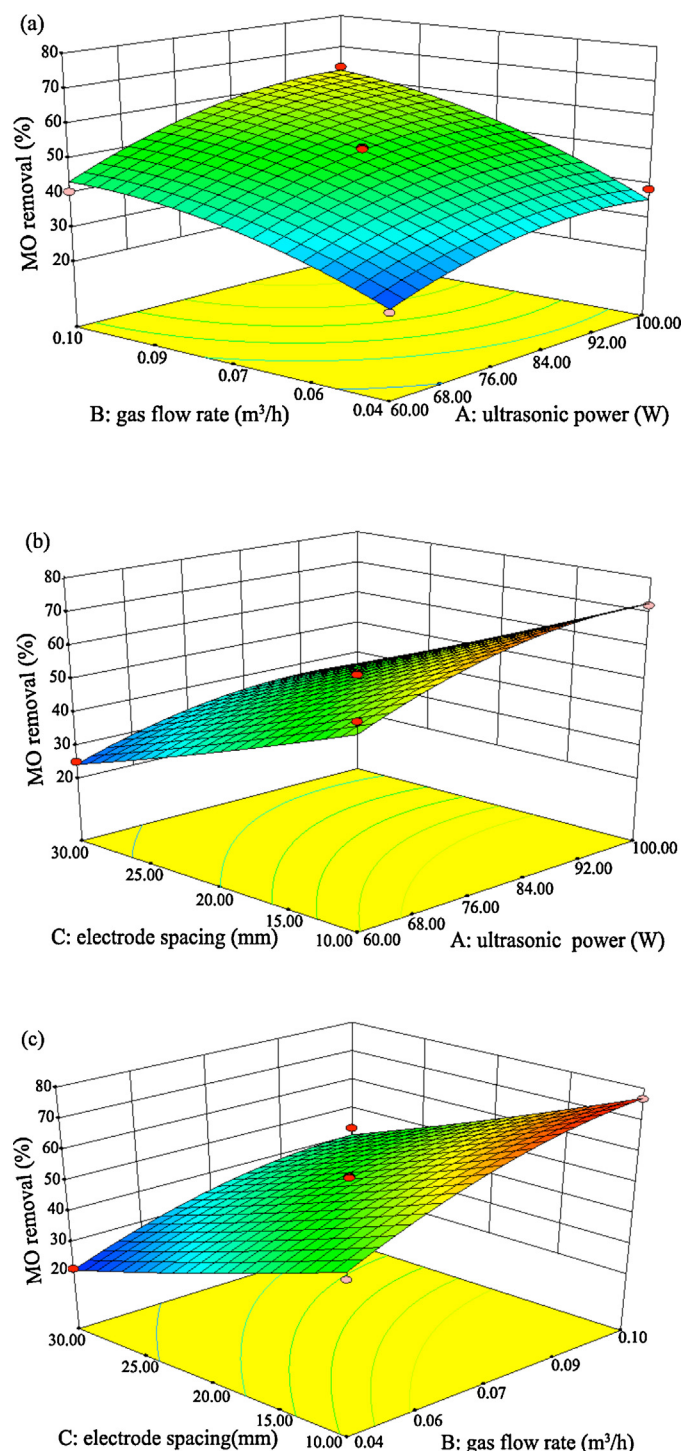


**Fig. 5.** Response surface plots for combined effect of (a) ultrasonic power and gas flow rate at constant electrode spacing of 20 mm, (b) ultrasonic power and electrode spacing at constant gas flow rate of 0.07 m<sup>3</sup>/h, and (c) gas flow rate and electrode spacing at constant ultrasonic power of 80 W on removal efficiency of MO.

could be obtained so that exciting and ionizing occur in the bubbles and/or water, which made it possible to produce more radicals for dye removal.

### 3.2.2. Effects of ultrasonic power and electrode spacing

The similar trend can be observed that the increased ultrasonic power resulted in the increasing dye removal efficiency (Figs. 4a,c and 3a,c), and decreased electrode spacing enhanced the dye

removal efficiency at constant gas flow rate ( $B = 0.07 \text{ m}^3/\text{h}$ ). Spark discharge occurred when the electrode spacing was 10 mm, and when the electrode spacing increased to be 20 mm and 30 mm, corona discharge was observed. The highest removal efficiency of both dyes was achieved when the electrode spacing was 10 mm, where the intensity of ultraviolet and shockwave, generated by electrohydraulic effects, was much higher than that of other cases, and ultraviolet photolysis and oxidation by active radical such as OH were enhanced [45]. As a result, higher removal efficiency was obtained.

### 3.2.3. Effects of gas flow rate and electrode spacing

Figs. 4b,c and 5b,c represent the conjugate effect of gas flow rate and electrode spacing at constant ultrasonic power ( $A = 80 \text{ W}$ ). It was evident that dye removal efficiency increases with gas flow rate and decreases with increasing electrode spacing within the experimental range. By analyzing the three dimensional response surface of combined effect of gas flow rate and electrode spacing, a maximum removal efficiency of MB and MO at 96.8% and 76.7% were achieved when gas flow rate and electrode spacing were  $0.10 \text{ m}^3/\text{h}$  and 10 mm, respectively, which was in accordance with the models. Yang *et al.* [45] achieved the highest degradation rate of AO by the liquid and gas phase discharges when the electrode distance was 10 mm.

### 3.3. Confirmation experiments

On the basis of RSM, the optimum levels of factors were predicted as gas flow rate of  $0.1 \text{ m}^3/\text{h}$ , electrode spacing 10 mm for all the dyes, and ultrasonic power 80 and 90 W for MB and MO. Under these conditions the removal efficiency was 96.8% and 82.6% for MB and MO, respectively. Furthermore, to support the optimized data as given numerical modeling under optimized condition, the confirmatory experiments were conducted with the parameters as suggested by the model and the removal efficiency for MB and MO was found to be 94.5% and 80.2%, respectively.

## 4. Conclusions

The objective of this study was to explore the optimum process conditions, using response surface methodology, required while using pulsed discharged plasma oxidation process to decolorize the MB and MO dyes from the simulated solutions and the following conclusions were achieved:

- (1) RSM by the BBD model were appropriate for determining the optimal conditions for MB and MO removal, understanding the relationships among the independent and response variables, and maximizing the process efficiency.
- (2) The optimal conditions were: gas flow rate  $0.1 \text{ m}^3/\text{h}$ , electrode spacing 10 mm for all the dyes, ultrasonic power 80 and 90 W for MB and MO. At optimum removal conditions, the predicted removal efficiency of pulsed discharged plasma reached 94.5% and 80.2% for MB and MO, respectively.
- (3) The pulsed discharged plasma oxidation process may be used as a rapid and low energy consumption method for removal of dyes from water.

## References

- [1] Kousha M, Daneshvar E, Sohrabi MS, Jokar M, Bhatnagar A. Adsorption of acid orange II dye by raw and chemically modified brown macroalga *Stoechospermum marginatum*. *Chem Eng J* 2012;192:67–76.
- [2] Li WH, Yue QY, Tu P, Ma ZH, Gao BY, Li JZ, et al. Adsorption characteristics of dyes in columns of activated carbon prepared from paper mill sewage sludge. *Chem Eng J* 2011;178:197–203.
- [3] Dizge N, Aydinler C, Demirbas E, Kobya M, Kara S. Adsorption of reactive dyes from aqueous solutions by fly ash: kinetic and equilibrium studies. *J Hazard Mater* 2008;150:737–46.
- [4] Zhang WX, Li HJ, Kan XW, Dong L, Yan H, Jiang ZW, et al. Adsorption of anionic dyes from aqueous solutions using chemically modified straw. *Bioresour Technol* 2012;117:40–7.
- [5] Kim T, Park C, Yang J, Kim S. Comparison of disperse and reactive dye removals by chemical coagulation and Fenton oxidation. *J Hazard Mater* 2004;112:95–103.
- [6] Kayan B, Gözmen B, Demirel M, Gizir AM. Degradation of acid red 97 dye in aqueous medium using wet oxidation and electro-Fenton techniques. *J Hazard Mater* 2010;177:95–102.
- [7] Gómez V, Larrechi MS, Callao MP. Kinetic and adsorption study of acid dye removal using activated carbon. *Chemosphere* 2007;69:1151–8.
- [8] Mahmoodi NM, Salehi R, Arami M. Binary system dye removal from colored textile wastewater using activated carbon: kinetic and isotherm studies. *Desalination* 2011;272:187–95.
- [9] Chafi M, Gourich B, Essadki AH, Vial C, Fabregat A. Comparison of electro-coagulation using iron and aluminium electrodes with chemical coagulation for the removal of a highly soluble acid dye. *Desalination* 2011;281:285–92.
- [10] Zhou XJ, Guo WQ, Yang SS, Ren NQ. A rapid and low energy consumption method to decolorize the high concentration triphenylmethane dye wastewater: operational parameters optimization for the ultrasonic-assisted ozone oxidation process. *Bioresour Technol* 2012;105:40–7.
- [11] Modirshahla N, Behnajady MA. Photooxidative degradation of malachite green (MG) by  $\text{UV}/\text{H}_2\text{O}_2$ : influence of operational parameters and kinetic modeling. *Dyes Pigments* 2006;70:54–9.
- [12] Berberidou C, Poullos L, Ps Kekoukoulotaki N, Mantzavinos D. Sonolytic, photocatalytic and sonophotocatalytic degradation of malachite green in aqueous solutions. *Appl Catal B-Environ* 2007;74:63–72.
- [13] Körbahti BK, Tanyolaç A. Electrochemical treatment of simulated textile wastewater with industrial components and Levafix Blue CA reactive dye: optimization through response surface methodology. *J Hazard Mater* 2008;151:422–31.
- [14] Zhang Z, Zheng H. Optimization for decolorization of azo dye acid green 20 by ultrasound and  $\text{H}_2\text{O}_2$  using response surface methodology. *J Hazard Mater* 2009;172:1388–93.
- [15] Guinea E, Brillas E, Centellas F, Cañizares P, Rodrigo MA, Sáez C. Oxidation of enrofloxacin with conductive-diamond electrochemical oxidation, ozonation and Fenton oxidation. A comparison. *Water Res* 2009;43:2131–8.
- [16] Santanab MHP, Silva LMD, Fretitas AC, Boodts JFC, Fernandes KC, Faria LAD. Application of electrochemically generated ozone to the discoloration and degradation of solutions containing the dye reactive orange 122. *J Hazard Mater* 2009;164:10–7.
- [17] Ai Z, Li J, Zhang L, Lee S. Rapid decolorization of azo dyes in aqueous solution by an ultrasound-assisted electrocatalytic oxidation process. *Ultrason Sonochem* 2010;17:370–5.
- [18] Du CM, Shi TH, Sun YW, Zhuang XF. Decolorization of Acid Orange 7 solution by gas-liquid arc discharge plasma. *J Hazard Mater* 2008;154:1192–7.
- [19] Magureanu M, Piroi D, Mandache NB, David V, Medvedovici A, Parvulescu VI. Degradation of pharmaceutical compound pentoxifylline in water by non-thermal plasma treatment. *Water Res* 2010;44:3445–53.
- [20] Dojčinović BP, Roglič GM, Obradović BM, Kuraica MM, Kostić MM, Nešić J, et al. Decolorization of reactive textile dyes using water falling film dielectric barrier discharge. *J Hazard Mater* 2011;192:763–71.
- [21] Sugiarto AT, Ito S, Ohshima T, Sato M, Skalný JD. Oxidative decoloration of dyes by pulsed discharge plasma in water. *J Electrostat* 2003;58:135–45.
- [22] Körbahti BK. Response surface optimization of electrochemical treatment of textile dye wastewater. *J Hazard Mater* 2007;145:277–86.
- [23] Ölmez T. The optimization of Cr(VI) reduction and removal by electrocoagulation using response surface methodology. *J Hazard Mater* 2009;162:1371–8.
- [24] Asgher M, Bhatti HN. Response surface methodology and central composite design of biosorption of reactive anthraquinone dyes by *Citrus sinensis* waste biomass. *Asian J Chem* 2010;22:7817–26.
- [25] Asgher M, Bhatti HN. Optimization of adsorption variables for removal of anionic dyes by *Citrus sinensis* biomass using response surface methodology. *Fresenius Environ Bull* 2011;20:2078–84.
- [26] Bian WJ, Song XH, Liu DQ, Zhang J, Chen XH. Actions of nitrogen plasma in the 4-chlorophenol degradation by pulsed high-voltage discharge with bubbling gas. *Chem Eng J* 2013;219:385–94.
- [27] Sadri MS, Alavi MMR, Arami M. Coagulation/flocculation process for dye removal using sludge from water treatment plant: optimization through response surface methodology. *J Hazard Mater* 2010;175:651–7.
- [28] Su SN, Nie HL, Zhu LM, Chen TX. Optimization of adsorption conditions of papain on dye affinity membrane using response surface methodology. *Bioresour Technol* 2009;100:2336–40.
- [29] Jain M, Garg VK, Kadirvelu K. Investigation of Cr(VI) adsorption onto chemically treated *Helianthus annuus*: optimization using response surface methodology. *Bioresour Technol* 2011;102:600–5.
- [30] Soloman PA, Ahmed BC, Velan M, Balasubramanian N, Marimuthu P. Augmentation of biodegradability of pulp and paper industry wastewater by electrochemical pre-treatment and optimization by RSM. *Sep Purif Technol* 2009;69:109–17.
- [31] Shafeeyan MS, Wan DWMA, Houshmand A, Arami-Niya A. The application of response surface methodology to optimize the amination of activated carbon for the preparation of carbon dioxide adsorbents. *Fuel* 2012;94:465–72.

- [32] Bezerra MA, Santelli RE, Oliveira EP, Villar LS, Escaleira LA. Response surface methodology (RSM) as a tool for optimization in analytical chemistry. *Talanta* 2008;76:965–77.
- [33] Balasubramanian N, Kojima T, Srinivasakannan C. Arsenic removal through electrocoagulation: kinetic and statistical modeling. *Chem Eng J* 2009;155:76–82.
- [34] Amini M, Younesi H, Bahramifar N. Biosorption of nickel(II) from aqueous solution by *Aspergillus niger*: response surface methodology and isotherm study. *Chemosphere* 2009;75:1483–91.
- [35] Vargas AMM, Martins AC, Almeida VC. Ternary adsorption of acid dyes onto activated carbon from flamboyant pods (*Delonix regia*): analysis by derivative spectrophotometry and response surface methodology. *Chem Eng J* 2012;195:173–9.
- [36] Tripathi P, Srivastava VC, Kumar A. Optimization of an azo dye batch adsorption parameters using Box–Behnken design. *Desalination* 2009;249:1273–9.
- [37] Silva JP, Sousa S, Goncalves I, Porter J, Ferreira-Dias. Modelling adsorption of acid orange 7 dye in aqueous solutions to spent brewery grains. *Sep Purif Technol* 2004;40:163–70.
- [38] Chatterjee S, Kumar A, Basu S, Dutta S. Application of response surface methodology for Methylene Blue dye removal from aqueous solution using low cost adsorbent. *Chem Eng J* 2012;181–182:289–99.
- [39] Meng RJ, Yu XJ. Investigation of ultrasound assisted regeneration of Ni-bentonite with response surface methodology (RSM). *Appl Clay Sci* 2011;54:112–7.
- [40] Wen YJ, Wu YH. Optimizing adsorption of Co(II) and Ni(II) by 13x molecular sieves using response surface methodology. *Water Air Soil Poll* 2012;223:6095–107.
- [41] Singh R, Chadetrik R, Kumar R, Bishnoi K, Bhatia D, Kumar A, et al. Biosorption optimization of lead(II), cadmium(II) and copper(II) using response surface methodology and applicability in isotherms and thermodynamics modeling. *J Hazard Mater* 2010;174:623–34.
- [42] Sarkar M, Majumdar P. Application of response surface methodology for optimization of heavy metal biosorption using surfactant modified chitosan bead. *Chem Eng J* 2011;175:376–87.
- [43] Lei LC, Zhang Y, Zhang XW, Shen YJ. Using a novel pulsed high-voltage gas-liquid hybrid discharge continuous reactor for removal of organic pollutant in oxygen atmosphere. *J Electrostat* 2008;66:16–24.
- [44] Li J, Sato M, Ohshima T. Degradation of phenol in water using a gas-liquid phase pulsed discharge plasma reactor. *Thin Solid Films* 2007;515:4283–8.
- [45] Yang B, Zhou MH, Lei LC. Synergistic effects of liquid and gas phase discharges using pulsed high voltage for dyes degradation in the presence of oxygen. *Chemosphere* 2005;60:405–11.